

concentration of plasminogen (31). The flexibility of the open form of plasmin may be important in its role in fibrinolysis. Since plasmin binds to fibrin through kringle 1, the protease domain, 554 amino acids away at the opposite end of the molecule, has a large radius within which to cleave fibrin (32). This would allow the open form, Lys-plasmin, to act catalytically on fibrin whereas the more rigid closed form of plasmin may act only stoichiometrically. Preliminary analysis of small-angle neutron scattering data from a variant of plasminogen missing the first 76 amino acids, Lys-plasminogen, and an NH₂-terminal fragment of plasminogen containing the first 3 kringles, indicates that their conformations were in the open form in the presence or absence of ligand binding.

REFERENCES AND NOTES

1. P. Wallen and B. Wiman, *Biochem. Biophys. Acta* **257**, 122 (1972).
2. L. Sottrup-Jensen, H. Claeys, M. Zajdel, T. E. Peterson, S. Magnusson, *Prog. Chem. Fibrinolysis Thrombolysis* **3**, 191 (1978).
3. F. J. Castellino, V. A. Ploplis, J. R. Powell, D. K. Strickland, *J. Biol. Chem.* **256**, 4778 (1981); V. A. Ploplis, D. K. Strickland, F. J. Castellino, *Biochemistry* **20**, 15 (1981); V. V. Novokhatny, S. A. Kudinov, P. L. Privalov, *J. Mol. Biol.* **179**, 215 (1984); M. Trexler and L. Patthy, *Proc. Natl. Acad. Sci. U.S.A.* **80**, 2457 (1983).
4. L. Patthy, *Cell* **41**, 657 (1985).
5. K. C. Robbins, L. Summaria, B. Hsieh, R. Shah, *J. Biol. Chem.* **242**, 2333 (1967).
6. G. Markus, J. L. De Pasquale, F. C. Wissler, *ibid.* **253**, 733 (1978).
7. S. Thorsen, *Biochim. Biophys. Acta* **251**, 363 (1975); E. Suenon and S. Thorsen, *Biochem. J.* **197**, 619 (1982); M. A. Lucas, L. J. Freeto, P. A. McKee, *J. Biol. Chem.* **258**, 4249 (1983); R. Bok and W. F. Mangel, *Biochemistry* **24**, 3279 (1985).
8. B. S. Knudsen, R. L. Silverstein, L. L. K. Leung, P. C. Harpel, R. L. Nachman, *Proc. Natl. Acad. Sci. U.S.A.* **261**, 10765 (1986).
9. E. F. Plow, D. E. Freaney, J. Plescia, L. A. Miles, *J. Cell Biol.* **103**, 2411 (1986).
10. B. Wiman and D. Collen, *Nature* **272**, 549 (1978).
11. U. Christensen and S. Mullertz, *Biochim. Biophys. Acta* **481**, 271 (1977); U. Christensen, *ibid.*, p. 638; S. W. Peltz, T. A. Hardt, W. F. Mangel, *Biochemistry* **21**, 2798 (1982).
12. N. Alkjaersig, *Biochem. J.* **93**, 171 (1964).
13. W. J. Brockway and F. J. Castellino, *Arch. Biochem. Biophys.* **151**, 494 (1972); B. N. Violand, R. Bryne, F. J. Castellino, *J. Biol. Chem.* **253**, 5395 (1978).
14. F. J. Castellino, W. J. Brockway, J. K. Thomas, H. Liao, A. B. Rawitch, *Biochemistry* **12**, 2787 (1973).
15. O. Glatter and O. Kratky, Eds., *Small Angle X-Ray Scattering* (Academic Press, London, 1982).
16. L. A. Compton and W. C. Johnson, Jr., *Anal. Biochem.* **155**, 155 (1986).
17. A. Guinier and B. Fournet, *Small Angle Scattering of X-Rays* (Wiley, New York, 1955).
18. U. K. Laemmler, *Nature* **227**, 680 (1972).
19. S. Panyin and R. Chalkley, *Arch. Biochem. Biophys.* **130**, 337 (1969).
20. P. B. Moore, *J. Appl. Cryst.* **13**, 168 (1980).
21. R. G. Kriste and R. C. Oberthur, in (15), pp. 387–432.
22. I. Sjöholm, B. Wiman, P. Wallen, *Eur. J. Biochem.* **39**, 471 (1973).
23. J. B. Siegel, W. E. Steinmetz, G. L. Long, *Anal. Biochem.* **104**, 160 (1980).
24. J. R. Powell, J. M. Beals, F. J. Castellino, *Arch. Biochem. Biophys.* **248**, 390 (1986).
25. T. F. Kumosinski and H. Pessen, *ibid.* **219**, 89 (1982).
26. G. Markus, J. L. Evers, G. H. Hobika, *J. Biol.*

- Chem.* **253**, 733 (1978).
27. H. Conrad, A. Mayer, H. P. Thomas, H. Vogel, *J. Mol. Biol.* **41**, 225 (1969).
28. R. C. McDonald, T. A. Steitz, D. M. Engelman, *Biochemistry* **18**, 338 (1979).
29. C. A. Pickover, D. B. McKay, D. M. Engelman, T. A. Steitz, *J. Biol. Chem.* **254**, 11323 (1979).
30. J. Monod, J. Wyman, J. P. Changeux, *J. Mol. Biol.* **12**, 88 (1965).
31. S. W. Peltz, T. A. Hardt, W. F. Mangel, *Biochemistry* **21**, 2798 (1982).
32. V. Ramakrishnan, L. Patthy, W. F. Mangel, unpublished results.
33. D. C. Livingston *et al.*, *Biochemistry* **20**, 4298 (1981); S. P. Leytus *et al.*, *ibid.*, p. 4307; S. W. Peltz, T. A. Hardt, W. F. Mangel, *ibid.* **21**, 2798 (1982); L. L. Melhado, S. W. Peltz, S. P. Leytus, W. F. Mangel, *J. Am. Chem. Soc.* **104**, 7299 (1982); R. Bok and W. F. Mangel, *Biochemistry* **24**, 3279 (1985).
34. D. Schneider and B. P. Schoenborn, in *Neutrons in*

- Biology*, B. P. Schoenborn, Ed. (Plenum, New York, 1984), pp. 119–142.
35. B. Jacrot and G. Zaccari, *Biopolymers* **20**, 2413 (1981).
36. J. C. Sutherland, E. J. Desmond, P. Z. Takacs, *Nucl. Instrum. Methods* **172**, 195 (1980); J. C. Sutherland, P. C. Keck, K. P. Griffin, P. Z. Takacs, *ibid.* **195**, 375 (1982).
37. We thank D. Schneider for help with the neutron scattering measurements, J. Sutherland for help with the circular dichroism measurements, and D. Toledo and J. Trunk for able technical assistance. This work was supported by the Office of Health and Environmental Research of the United States Department of Energy. The High Flux Beam Reactor and the National Synchrotron Light Source are supported by the Division of Chemical Sciences and the Division of Materials Sciences, Office of Basic Energy Sciences, United States Department of Energy.

13 November 1989; accepted 6 February 1990

Two-Photon Laser Scanning Fluorescence Microscopy

WINFRIED DENK,* JAMES H. STRICKLER, WATT W. WEBB

Molecular excitation by the simultaneous absorption of two photons provides intrinsic three-dimensional resolution in laser scanning fluorescence microscopy. The excitation of fluorophores having single-photon absorption in the ultraviolet with a stream of strongly focused subpicosecond pulses of red laser light has made possible fluorescence images of living cells and other microscopic objects. The fluorescence emission increased quadratically with the excitation intensity so that fluorescence and photobleaching were confined to the vicinity of the focal plane as expected for cooperative two-photon excitation. This technique also provides unprecedented capabilities for three-dimensional, spatially resolved photochemistry, particularly photolytic release of caged effector molecules.

WE REPORT THE APPLICATION OF two-photon excitation of fluorescence (1) to laser scanning microscopy (LSM) (2). In LSM, the laser is focused to a diffraction-limited beam waist <1 μm in diameter and is raster-scanned across a specimen. Confocal LSM provides depth discrimination and improves spatial resolution within the plane of focus by forming the image through the same scanning optics used for illumination and through a pinhole placed in front of the detector, which acts as a spatial filter to select emission from the plane of focus (2). Very good laser scanning micrographs have been obtained with the use of fluorescent markers that absorb and emit visible light (3). Confocal scanning images with fluorophores and fluorescent chemical indicators that are excited by the ultraviolet (UV) part of the spectrum have not appeared, however, largely because of the lack of suitable microscope lenses, which must be chromatically corrected and transparent for both

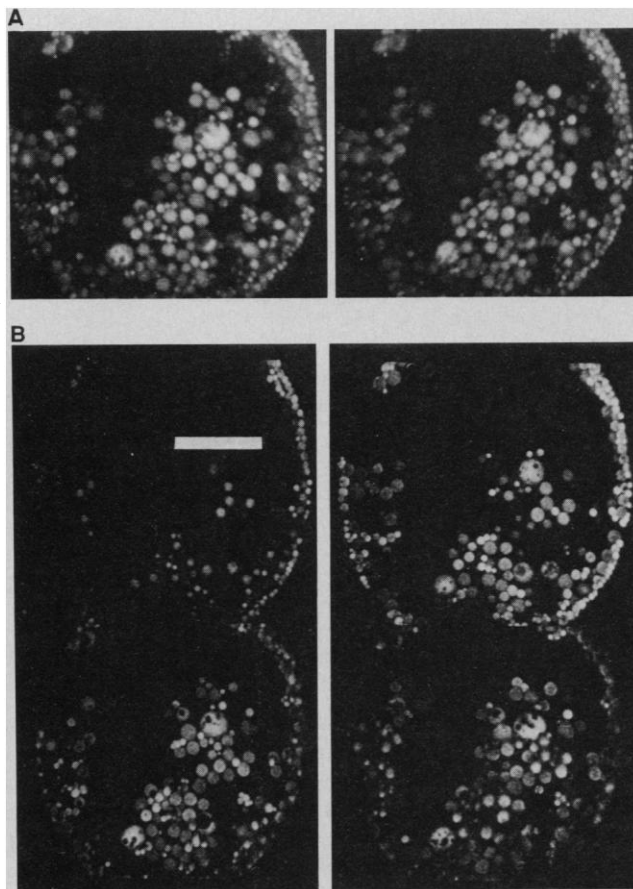
absorption and emission wavelengths (4, 5). Anticipated photodamage to living cells and the limitations of UV lasers have also inhibited this approach.

Two-photon molecular excitation (1, 6) is made possible by the very high local instantaneous intensity provided by the tight focusing in an LSM combined with the temporal concentration of a femtosecond pulsed laser. With a colliding-pulse, mode-locked dye laser (7) (CPM) producing a stream of pulses with a pulse duration (τ_p) of about 100 fs at a repetition rate (f_p) of about 80 MHz, the probability becomes appreciable for a dye molecule to absorb two long-wavelength (λ_{CPM}) photons simultaneously, thus combining their energy in order to reach its excited state. Assuming a typical two-photon cross section (8) of $\delta = 10^{-58}$ m⁴·s per photon with the above pulse parameters and the beam focused by a lens of numerical aperture $A \approx 1.4$, we calculated that an average incident laser power (p_0) of ~50 mW would saturate the fluorescence output at the limit of one absorbed photon pair per pulse per fluorophore (9). The fluorescence emission could be increased, however, if the pulse repetition frequency were increased to the inverse fluorescence

School of Applied and Engineering Physics, Department of Physics, Cornell University, Ithaca, NY 14853.

*Present address: IBM Forschungslaboratorium, Säumerstrasse 4, CH-8803 Rüschlikon, Switzerland.

Fig. 1. (A) A stereo image pair is synthesized from a stack of six cross sections (xy sections) with an axial (z) increment of $3 \mu\text{m}$. Blue ($380 \text{ nm} \leq \lambda \leq 445 \text{ nm}$) fluorescence excited by two-photon (630 nm) absorption was detected to record these images of a cluster of fluorescent beads with an LSM but with its confocal pinhole fully opened. The latex beads are volume-stained with the dye Coumarin 138 and have their measured absorption and emission maxima at 365 and 415 nm , respectively. The data comprise ten averages for each section with no background subtraction or image enhancement. The total time to acquire the data was less than 2 min . (B) The topmost four of the images, xy sections, used to synthesize the stereo pair in (A). Scale bar, $50 \mu\text{m}$.



lifetime of typically $\tau_f^{-1} \approx 10^9 \text{ s}^{-1}$. For comparison, one-photon fluorescence saturation occurs at incident powers of about 3 mW (4).

To illustrate (Fig. 1) the depth discrimination achieved in these first experiments, we generated a stereo image pair from a stack of images of a cluster of fluorescent latex beads $9 \mu\text{m}$ in diameter, which are normally excited by UV light at $\lambda \approx 365 \text{ nm}$ (Fluoresbrite BB; Polysciences). The images were recorded with a standard LSM (Bio-Rad; MRC 500) with its continuous-wave argon ion laser illuminator replaced by a 25-mW CPM ($\lambda \approx 630 \text{ nm}$) (Clark Instruments, Pittsford, New York). Throughput measurements (4) indicate that $\sim 3 \text{ mW}$ reached the object plane. An emission filter, passing wavelengths from 380 to 445 nm , was used, and the detector aperture was opened to its limit to reduce the optical sectioning effect that would result from a small confocal aperture.

The blue fluorescence power detected from areas inside individual beads $\sim 10 \mu\text{m}$ in diameter increased with the square of the excitation power, which we adjusted by changing neutral density filters in the excitation beam. Fluorescence power measurements over a two-decade range with background corrected only for scattering, mea-

sured in an area outside the bead, all fell within $\sim 10\%$ of a logarithmic best-fit straight line, which has a slope of 2.06 ± 0.09 . This result clearly indicates two-photon excitation. We estimated the excitation cross section to be $5 \times 10^{-58} \text{ m}^4\text{-s}$ per photon (within a factor of 3) by taking into account the dye concentration in the beads, the optical throughput of the LSM, τ_p , f , A , and p_0 and using equation 4 of (10). This value is comparable to previously measured

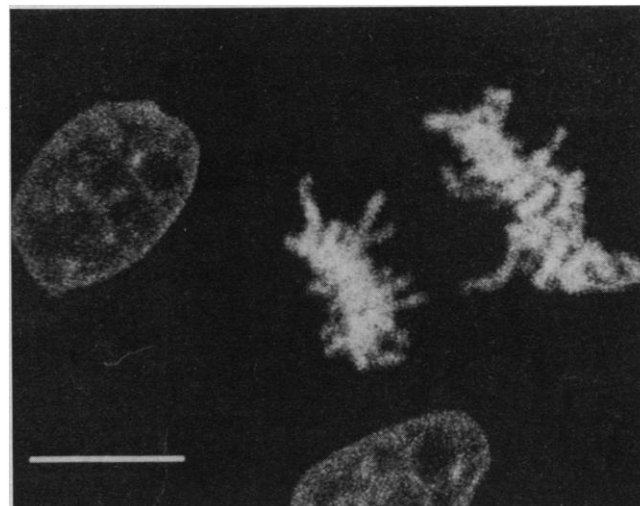
values for similar dyes (8, 11).

A scanned image of chromosomes in dividing cells (LLC-PK-1; American Type Culture Collection) stained by cellular DNA labeling with a UV excitable fluorescent stain (Hoechst 33258) is shown in Fig. 2. The image acquisition time, 13 s , was short as compared to the bleaching time of several minutes. No degradation was apparent in the micromorphology of these live cells even after illumination by the scanning laser for several minutes.

Photobleaching during protracted scanning occurred only in a slice about $2 \mu\text{m}$ thick around the focal plane, as is evident from the horizontal band of reduced brightness bleached out of a fluorescent bead (Fig. 3) that was scanned for 6 min at a constant focal plane position. Similar localization of bleaching was observed in the fluorescently stained cell nuclei. This localization illustrates a distinct advantage of two-photon excitation over single-photon excitation, where the entire specimen is bleached even when only a single plane is imaged. For one-photon excitation, bleaching in both scanning and broad-field microscopy (at least in a regime of intensity-independent bleaching cross section) (12) depends on the time-averaged excitation intensity, which does not vary along the axial or z direction. For two-photon excitation, on the other hand, bleaching depends on the time-averaged square of the intensity, which falls off strongly above and below the focal plane (as $1/z^2$ for large z).

The quadratic dependence of signal on excitation intensity is responsible for another advantage of two-photon excitation: it provides an optical sectioning effect, even with a detector such as a charge-coupled device (CCD) array which views the whole field, without a pinhole as a spatial filter. This sectioning effect (Fig. 3) is similar to

Fig. 2. A two-photon excited fluorescence image generates an optical section through chromosomes of live cultured pig kidney cells (LLC-PK-1), stained with a viable DNA stain (Hoechst 33258) by incubation in a solution (5 mg/liter) for 5 min at 37°C . Two cells are seen in interphase, and one cell is seen in anaphase. The image was recorded with a fully open detector pinhole and comprises a 13-frame average (total time, 13 s). Scale bar, $10 \mu\text{m}$.



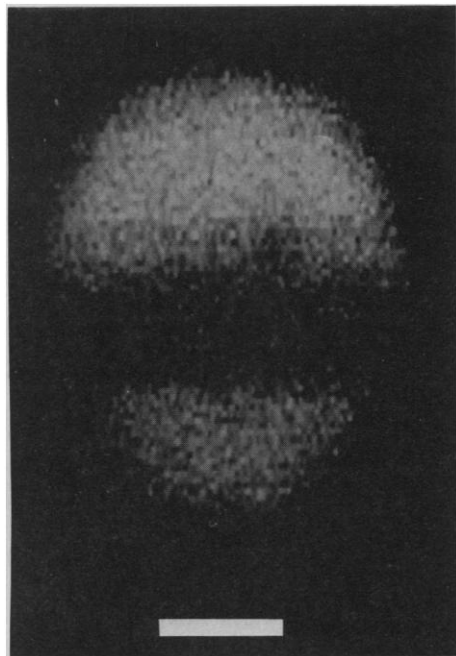


Fig. 3. Two-photon photobleaching in a latex bead is confined to the plane of focus. A section perpendicular to the focal plane (xz section) of a 6- μm latex bead that was continually imaged for 6 min at full excitation power with a small image field (26 μm by 17 μm) with the focus slightly below the center of the bead. The dark zone just below the center coincides with the location of the focal plane. The oblong shape of the image of a bead, which is in fact spherical, is due to refractive distortion. The total dose of red laser light was $\sim 2 \text{ mJ}/\mu\text{m}^2$. We estimated that at least several thousand photons were emitted from each fluorophore before it bleached. Scale bar, 2 μm .

that achieved with one-photon excitation in conjunction with an optimal confocal pinhole. But two-photon excitation avoids the serious problems associated with chromatic aberration in the objective lens (4, 5) and pinhole throughput losses (4) that plague confocal LSM.

Two-photon photolysis can be used for fast and localized release of biologically active chemicals (13) such as caged Ca^{2+} , H^+ , nucleotides, and neurotransmitters (14). For example, if caged neurotransmitters (15) are released by the scanning beam, the whole-cell transmembrane current might be used as the contrast-generating mechanism to map the distribution of receptor activity for those transmitters on the cell surface. We demonstrated the feasibility of two-photon cage photolysis by irradiating DMNPE {3-O-[1-(2-nitrophenyl)ether]ester} caged adenosine triphosphate (ATP) (33 mM) [Molecular Probes, Eugene, Oregon) with the CPM focused to a beam waist diameter of $\sim 10 \mu\text{m}$. Photolysis yields of $\sim 10^{-11}$ mol of ATP were measured with the use of a luciferin bioluminescence assay (Calbiochem, San Diego, California). Typically $\sim 10\%$ of

the caged ATP in an aliquot volume of $\sim 10^7 \mu\text{m}^3$ was photolyzed in the illumination volume of $\sim 10^4 \mu\text{m}^3$ during ~ 600 s. This result implies potential cage release times < 1 s in the $10^4\text{-}\mu\text{m}^3$ illumination volume and presumably much faster photolysis with stronger focusing in smaller volumes.

Because two-photon excitation provides access by visible light to excitation energies corresponding to single UV photon excitation, a whole new class of fluorophores and fluorescent indicators (16) such as Indo-1 for Ca^{2+} , Mag-Indo-1 for Mg^{2+} , SBFI for Na^+ , and PBFI for K^+ becomes accessible to three-dimensional resolved LSM. Although two-photon cross sections are not yet known for many of these compounds and different selection rules apply to two-photon absorption (17), molecular asymmetry often allows both one-photon and two-photon transitions into the same excited state (3). Reports of two-photon excitation cross sections $> 10^{-56} \text{ m}^4\text{-s}$ per photon, with excitation spectra shifted, however, from the one-photon spectra, suggest chromophores suited to two-photon LSM (18). Visible fluorescence was observed from ~ 10 mM solutions of Indo-1, fura-1, Hoechst 33258, Hoechst 33342, dansyl hydrazine (Molecular Probes) (16), Stilbene 420 (Exciton Chemical Company, Dayton, Ohio), and several coumarin dyes upon excitation by a CMP weakly focused to a beam waist 25 μm in diameter, and two-photon excited LSM fluorescence images of microcrystals of dansyl hydrazine and Coumarin 440 were recorded.

Three-dimensional optical memory devices relying on multiphoton processes in

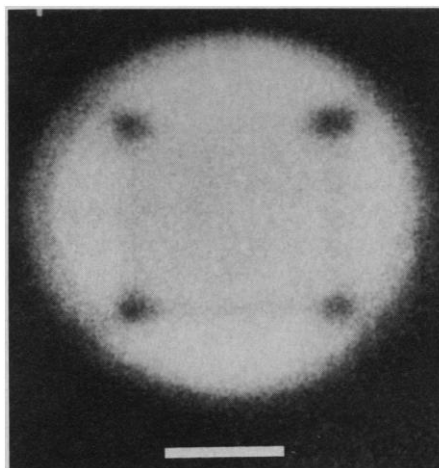


Fig. 4. A two-photon bleached pattern is shown by an xy section through a fluorescently stained 6- μm latex bead (compare Fig. 3). To bleach a single focal volume by $\sim 90\%$, irradiation for about 1 s was required. The four overbleached points were exposed for approximately 13 s each. Scale bar, 2 μm .

two intersecting beams for writing and reading operations have recently been proposed (19). Simplicity and maximal information packing density may favor a scheme based on the use of a single beam. Multiphoton processes would then be localized to the high-intensity region at the focus. In fact, we have demonstrated two-photon bleaching of microscopic patterns generated with an LSM inside fluorescent beads (Fig. 4), which constitutes a high-density write-once memory that is readable at least 10^3 times with present fluorophores.

Practical realization of two-photon laser scanning fluorescence microscopy for biological and other applications has been demonstrated. Two-photon excited fluorescence LSM provides inherent three-dimensional resolution comparable to that of confocal LSM. Use of a confocal pinhole in conjunction with two-photon excitation further improves resolution along all three axes. Background that is linear in the excitation intensity can be eliminated by scaled subtraction of images recorded at different input powers. The time required to record our images (about 10 s for a laser power of 3 mW at the focal plane) should be easily reduced by a factor of at least 10 and the image quality greatly improved by the increase in the optical throughput alone.

Photobleaching, and presumably photodynamic damage, are confined to the vicinity of the focal plane (Figs. 3 and 4) in the two-photon case. This is expected to provide a considerable advantage over both confocal LSM and area detector imaging for the acquisition of data for three-dimensional reconstruction, because UV photodamage to cells and fluorophores will be confined to the volume from which information is actually collected. This principle also allows sharp localization of purposeful photochemical processes, such as photolysis and photoactivation, within the focal volume.

The physiological advantage of two-photon photoexcitation for fluorescence studies of living cells remains to be evaluated. We can make only qualitative statements about cell viability on the basis of morphology comparisons of our visual observations after two-photon scanning excitation of the DNA stain and after wide-field excitation with UV from a conventional mercury arc illuminator. Although a few minutes of exposure to the mercury arc produced severe morphological changes including central rounding with extensive retraction fibers, the exposure to the two-photon excitation at roughly the same energy per cell produced no visible morphological change. It has not been determined whether mitosis was inhibited. Use of infrared lasers for two-photon excitation of chromophores ordinarily excited

with visible light may avoid the usual photo-dynamic perturbation entirely and facilitate protracted fluorescence observations of living cells.

REFERENCES AND NOTES

- W. L. Peticolas, J. P. Goldsborough, K. E. Reickhoff, *Phys. Rev. Lett.* **10**, 43 (1963).
- T. Wilson and C. Sheppard, *Theory and Practice of Scanning Optical Microscopy* (Academic Press, New York, 1984).
- J. G. White, W. B. Amos, M. Fordham, *J. Cell Biol.* **105**, 41 (1987).
- K. S. Wells, D. R. Sandison, J. H. Strickler, W. W. Webb, in *Handbook of Biological Confocal Microscopy*, J. Pawley, Ed. (Plenum, New York, 1990); W. W. Webb, K. S. Wells, D. R. Sandison, J. Strickler, in *An International Conference on Digitized Video Microscopy*, B. Herman and K. Jacobson, Eds. (Liss, New York, in press).
- H. E. Keller, in *Handbook of Biological Confocal Microscopy*, J. Pawley, Ed. (Plenum, New York, 1990).
- M. Göppert-Mayer, *Ann. Phys. (Paris)* **9**, 273 (1931).
- J. A. Valdemanis and R. L. Fork, *IEEE J. Quantum Electron.* **OE-22**, 112 (1986); F. W. Wise, I. A. Walsmsley, C. L. Tang, *Opt. Lett.* **13**, 129 (1988).
- J. P. Hermann and J. Ducuing, *Phys. Rev. A* **5**, 2557 (1972).
- The number n_a of photons absorbed per fluorophore per pulse depends on τ_p , f_p , p_0 , and A , as

$$n_a \approx \frac{p_0^2 \delta}{\tau_p f_p^2} \left(\frac{A^2}{2\hbar c \lambda} \right)^2$$
 where c is the speed of light, \hbar is the Planck quantum of action, and δ is the two-photon absorption cross section; saturation is neglected, and the paraxial approximation is assumed.
- R. R. Birge, *Acc. Chem. Res.* **19**, 138 (1986).
- L. Parma and N. Onemetto, *Chem. Phys. Lett.* **54**, 541 (1978).
- R. Y. Tsien and A. Waggoner, in *Handbook of Biological Confocal Microscopy*, J. Pawley, Ed. (Plenum, New York, 1990).
- If certain chemical bonds are photolyzed, an inactive ("caged") derivative of a molecule can be converted into its active form. See (14, 15).
- J. A. McCray and D. R. Trentham, *Annu. Rev. Biophys. Biophys. Chem.* **18**, 239 (1989).
- T. Milburn et al., *Biochemistry* **28**, 49 (1988).
- R. P. Haugland, *Molecular Probes Handbook of Fluorescent Probes and Research Chemicals* (Molecular Probes, Eugene, OR, 1989).
- L. Goodman and R. P. Rava, *Acc. Chem. Res.* **17**, 250 (1984).
- S. M. Kennedy and F. E. Lytle, *Anal. Chem.* **58**, 2643 (1986).
- D. A. Parthenopoulos and P. M. Rentzepis, *Science* **245**, 843 (1989).
- We thank F. Wise and R. Proctor for advice, aid, and use of their CPM. S. Wells provided advice and data on the LSM, T. Ryan some digital image reductions, and E. Kable the stained cultured cells. This research is a project of the NIH Developmental Resource for Biophysical Imaging Opto-electronics (RR04224) and the NSF National Instrumentation Facility for Optical Microscopy (DIR-8800278), and was also supported under NSF grants BBS 8714069 and DMB-8609084. W.D. was an IBM predoctoral fellow, J.H.S. a NIH trainee, and W.W.W. an NIH Fogarty Scholar during part of the time during which this research was conducted.

27 October 1989; accepted 8 February 1990

Association of Human Papillomavirus Types 16 and 18 E6 Proteins with p53

BRUCE A. WERNES, ARNOLD J. LEVINE, PETER M. HOWLEY

Human papillomavirus type 16 (HPV-16) is a DNA tumor virus that is associated with human anogenital cancers and encodes two transforming proteins, E6 and E7. The E7 protein has been shown to bind to the retinoblastoma tumor suppressor gene product, pRB. This study shows that the E6 protein of HPV-16 is capable of binding to the cellular p53 protein. The ability of the E6 proteins from different human papillomaviruses to form complexes with p53 was assayed and found to correlate with the *in vivo* clinical behavior and the *in vitro* transforming activity of these different papillomaviruses. The wild-type p53 protein has tumor suppressor properties and has also been found in association with large T antigen and the E1B 55-kilodalton protein in cells transformed by SV40 and by adenovirus type 5, respectively, providing further evidence that the human papillomaviruses, the adenoviruses, and SV40 may effect similar cellular pathways in transformation.

THE HUMAN PAPILLOMAVIRUSES (HPVs) that infect the anogenital area can be separated on the basis of their clinical associations into two distinct groups. The first group, including HPV-6 and HPV-11, is generally associated with benign anogenital warts that infrequently progress to cancer and have been referred to as "low-risk" viruses. The "high-risk" group, including HPV-16 and HPV-18, is associated with lesions that are at high risk for malignant progression and with almost all cervical carcinomas (1). The ability of cloned viral genomes derived from the high-risk but not the low-risk HPVs to transform cells in culture suggests that these papillomavirus

types have an etiologic role in these tumors (2). In cervical carcinomas and in cell lines derived from cervical carcinomas, the E6 and E7 open reading frames (ORFs) of the high-risk HPVs are regularly found to be intact and actively transcribed, implicating the E6 and E7 genes in the malignant phenotype (3, 4). Support for this role is provided by genetic analyses that establish the requirement for both E6 and E7 for the efficient transformation of primary human squamous epithelial cells by HPV-16 (5).

DNA tumor viruses appear to exert some of their proliferative and oncogenic effects on the host cell through interactions with cellular proteins. The HPV-16 E7 protein, like SV40 large T antigen (6) and adenovirus E1A (7), is capable of binding pRB (8). The E7 proteins of both high-risk and low-risk genital type HPVs have been shown to bind to pRB (9). The E7 proteins of HPV-6

and HPV-11 bind with 20-fold and 5-fold lower affinities, respectively, than the E7 proteins of HPV-16 and HPV-18. Thus, the ability of E7 to bind pRB *per se* does not alone allow for the qualitative discrimination between the different biologic properties of these viruses. The oncogenic potential of the E6 protein encoded by the high-risk HPVs has been revealed in transformation studies with primary human cells (5, 10). Like the E7 protein, which is 98 amino acids in size, the E6 protein is small (158 amino acids), and it is likely that its transforming properties may also result from the ability to form complexes with and potentially modulate the activity of critical cellular proteins that regulate cellular growth and differentiation. Since the large T antigen of SV40 (11, 12) and the E1B 55-kD protein of adenovirus 5 (13) can form a complex with the p53 protein, we explored the possibility that HPV-16 E6 also encodes a p53 binding protein. Although formerly classified as a dominantly acting oncogene (14–16) wild-type p53 has been shown to have tumor suppressor properties (17–22).

The possibility that HPV-16 E6 or E7 bound to or interacted with p53 was assessed by an *in vitro* binding assay similar to that used to show E7 complex formation with pRB (8). For these experiments, labeled HPV-16 E6 and E7 proteins synthesized in rabbit reticulocyte lysates were mixed with lysates of unlabeled mouse F9 cells. The F9 cells contain wild-type p53 protein that, unlike mutant p53 protein, binds efficiently to SV40 large T antigen (19, 23). The mixture was incubated with antibodies directed against p53, and the immunoprecipitate was analyzed for the

B. A. Werness and P. M. Howley, Laboratory of Tumor Virus Biology, National Cancer Institute, Bethesda, MD 20892.

A. J. Levine, Department of Biology, Princeton University, Princeton, NJ 08540.